REPORT DOCUMENTATION PAGE

Form Approved OMB NO. 0704-0188

1. REPORT DATE (DD-MM-YYYY)	2. REPORT TYPE	3. DATES COVERED (From - To)
12-01-2010	Final Report	15-Jul-2006 - 31-Dec-2009

4. TITLE AND SUBTITLE

Multispectral Visible/Infrared Sensors based on Polymer-Metal Nanocomposites

5a. CONTRACT NUMBER
W911NF-06-1-0295

5b. GRANT NUMBER

5c. PROGRAM ELEMENT NUMBER
611102

6. AUTHORS
Hergen Eilers

5d. PROJECT NUMBER

5e. TASK NUMBER

5f. WORK UNIT NUMBER

7. PERFORMING ORGANIZATION NAMES AND ADDRESSES
Washington State University
Office Of Grant & Research Development
French Administration Bldg.
Pullman, WA 99163 -

8. PERFORMING ORGANIZATION REPORT NUMBER

9. SPONSORING/MONITORING AGENCY NAME(S) AND ADDRESS(ES)
U.S. Army Research Office
P.O. Box 12211
Research Triangle Park, NC 27709-2211

10. SPONSOR/MONITOR'S ACRONYM(S)
ARO

11. SPONSOR/MONITOR'S REPORT NUMBER(S)
49585-EL.2

12. DISTRIBUTION AVAILIBILITY STATEMENT
Approved for Public Release; Distribution Unlimited

13. SUPPLEMENTARY NOTES
The views, opinions and/or findings contained in this report are those of the author(s) and should not contrued as an official Department of the Army position, policy or decision, unless so designated by other documentation.

14. ABSTRACT
P3HT:PCBM based reference and active device structures, as well as Grätzel-cell type based reference and active structures were fabricated and their optical and electrical properties measured. The reference structures for both types showed the expected optical absorption in the visible wavelength range and the electrical performance was similar to results reported in the scientific literature. All of the active devices showed increased optical absorption in the near- infrared. The active device structures based on P3HT:PCBM showed an electrical short and no I-V

15. SUBJECT TERMS
Polymer-metal nanocomposites, P3HT/Ag nanocomposites, Electronic Structure, XPS/UPS

16. SECURITY CLASSIFICATION OF:			17. LIMITATION OF ABSTRACT	15. NUMBER OF PAGES	19a. NAME OF RESPONSIBLE PERSON
a. REPORT	b. ABSTRACT	c. THIS PAGE			Hergen Eilers
UU	UU	UU	UU		19b. TELEPHONE NUMBER: 509-358-7681

Multispectral Visible/Infrared Sensors based on Polymer-Metal Nanocomposites

W911NF-06-1-0295

Final Progress Report

January 2010

Prepared for:

Dr. William Clark
Department of the Army
US Army Research, Development and Engineering Command
U. S. Army Research Office
P.O. BOX 12211
Research Triangle Park, NC 27709-2211
Phone: (919) 549-4314
Fax: (919) 549-4310
Email: william.w.clark@us.army.mil

Prepared by:

Hergen Eilers, Ph.D.
Washington State University
Institute for Shock Physics
Applied Sciences Laboratory
PO Box 1495
Spokane, WA 99210-1495
Phone: (509) 358-7681
Fax: (509) 358-7627
Email: eilers@wsu.edu

I. FOREWORD

The originally proposed research for this project was to fabricate broadband multispectral sensor materials made from thin–film polymer–metal nanocomposites with a metal concentration near the percolation threshold, with the objective to fabricate a sensor device with a spectral response ranging from the visible (~400 nm) to the mid-wave infrared (~5,000 nm and beyond).

Due to budget constraints, and per ARO's suggestion, the effort was focused on the relevant materials characterization only. The materials research aspects have been reported in the previous interim reports and publications. Based on these results, we were able to fabricate and characterize a few initial device structures during the last 4 months of the no-cost extension. Also, per agreement with the program manager, we fabricated and characterized some Grätzel-cell type structures that use nanophase silver instead of molecular dyes.

II. TABLE OF CONTENTS

I. Foreword 2

II. Table of Contents 2

III. List of Appendixes 2

IV. Statement of the problem studied 3

V. Summary of the most important results 4

a. Materials Research 4

i. Electrical Properties of n-Ag films 4

ii. Electrical Properties of n-Ag/polymer composites 4

iii. Thermal Evaporation of P3HT and PCBM 5

iv. Interfacial electronic structure of P3HT thin films on Ag substrates 6

v. Interfacial electronic structure of Ag/P3HT nanocomposites 6

b. Initial device performance 7

c. Conclusions 8

VI. Bibliography 8

VII. Appendix 9

III. LIST OF APPENDIXES

Device structure results

IV. STATEMENT OF THE PROBLEM STUDIED

The Army requires affordable high-resolution and high-sensitivity sensors for a variety of applications, including target recognition and acquisition, identification, and missile surveillance. Sensors convert incoming electromagnetic radiation into electrical signals. The spectral range that can be detected with a particular sensor depends on the sensor material used. Many applications, including the detection of missiles during the boost phase, require sensing in at least two parts of the electromagnetic spectrum to make a positive identification, and thus multiple sensors in the monitoring devices. In addition to the spectral requirements, it is desirable to use sensors that do not require cryogenic cooling, since that leads to additional expenses as well as cumbersome handling and maintenance of the sensors.

Over the last few years, a new class of materials, so-called nanocomposites – consisting of metallic nanoparticles embedded in dielectric matrices, has been investigated. These materials have interesting optical and electronic properties.[1-3] They are capable of absorbing light over a broad wavelength range and of generating a photocurrent,[4] making them suitable for sensor and photovoltaic applications, see Figures 1a and 1b.

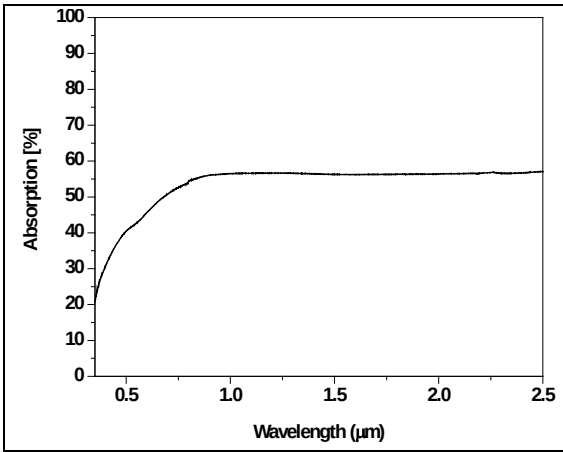

Figure 1a. Absorption profile of a Teflon AF/Ag composite with about 60% metal content.[1]

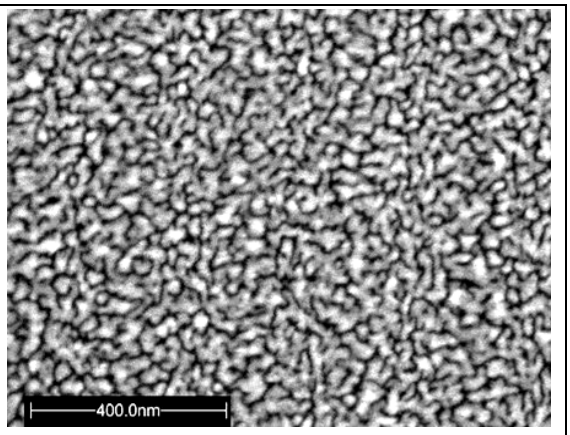

Figure 1b. SEM image of a Teflon AF / Ag composite with about 60% metal content.[1]

A typical polymer-metal nanocomposite for sensor applications would consist of metallic nanoparticles such as silver (Ag), gold (Au), or copper (Cu) embedded in a dielectric matrix such as electron transporting and hole-transporting organic semiconducting polymers. These polymer-metal nanocomposites absorb light by exciting surface plasmons (oscillations of electron clouds) in the metals. The resonance frequency of this oscillation depends on the size of the metal particles, the shape of the metal particles, and the type of metal. When the frequency of the incoming light is close to the resonance frequency of the surface plasmon, strong absorption can occur.[5]

For the sensor application, a polymer thin film with embedded metallic nanoparticles of various shapes and sizes is used. A broad distribution of shapes and sizes results in a broad distribution of resonance frequencies. When the filler concentration of the metallic nanoparticles is close to the percolation threshold (continuous metallic pathway), whole clusters of metallic nanoparticles can start to oscillate, and surface plasmons will be localized within the cluster. Surface plasmons, spread over larger clusters, will absorb at longer wavelengths than surface plasmons on

individual nanoparticles. A collection of clusters with varying sizes will therefore absorb light over a broad spectral range.[7]

The oscillations of the electron clouds can lead to strongly enhanced electric fields within the inter-particle gaps. For silver nanoparticles, the internal field can exceed the external field by up to a factor of 50.[5] This strong internal electric field can eject excited electrons from the surface plasmons. These electrons will be captured by the surrounding electron-transporting material such as PCBM, while the holes in the metal nanoparticles are transferred to hole-transporting materials such as P3HT.

V. SUMMARY OF THE MOST IMPORTANT RESULTS

a. Materials Research

i. Electrical properties of n-Ag films

The electrical conductance of silver films was investigated as a function of film thickness and under various applied external electrical fields. Three conductivity zones with distinct microstructures were observed: dielectric (film consists of isolated particle islands), transition (film consists of percolated metallic network), and metallic (film consists of a metallic continuum). The electron transport in the dielectric zone is governed by an activated tunneling process, while the electron transport in the metallic zone can be described by Ohm's law. The transition zone between the dielectric and the metallic zones is characterized by the appearance of the first conductive pathway across the film. An external electrical field applied across the film can shift the onset of this transition zone to lower film thicknesses. This shift is due to the change of activation energy. The slope in the transition zone can be tuned by varying the deposition rate.

ii. Electrical properties of n-Ag/polymer composites

The electrical properties of Ag/Teflon AF thin film nanocomposites were studied under an applied external constant potential as a function of film thickness at various metal loadings.

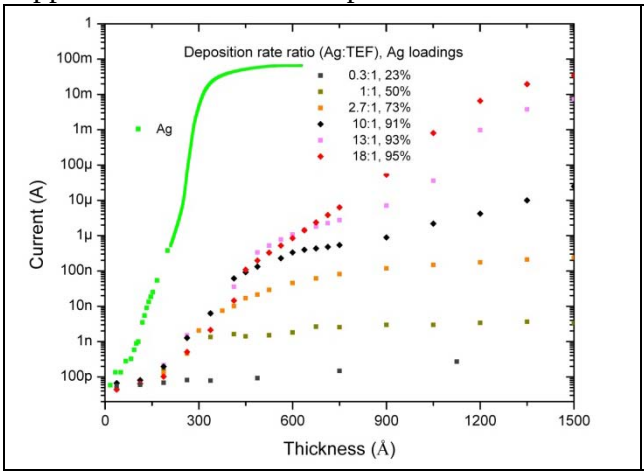

Figure 2a. In-situ measurements of electrical current at 1 V as a function of film thickness for various metal concentrations in Teflon-AF/ silver nanocomposites and the pure metal film.

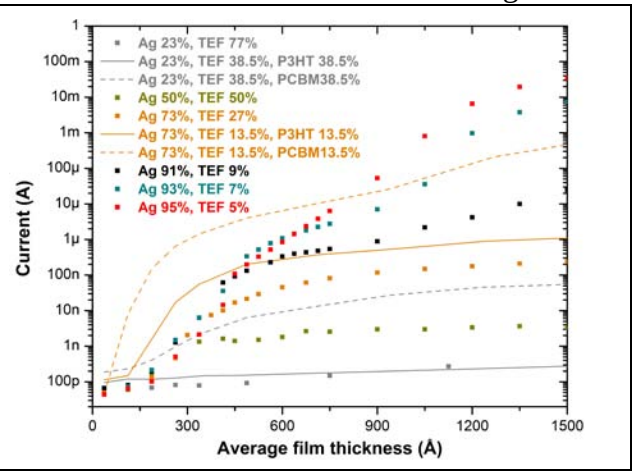

Figure 2b. Electrical conductance of Ag/Teflon AF, Ag/Teflon AF/P3HT and Ag/Teflon-AF/PCBM nanocomposite films as a function of film thickness with various metal loadings under 1 V external potential.

The electrical properties are directly dependent on the morphology of the silver nanoparticles embedded in the Teflon AF matrix. Composite films with a very low metal concentration and metallic nanoparticles well dispersed within the polymer matrix, show dielectric characteristics. Initially isolated nanoparticles in composite films with a moderate metal loading are able to coalesce into fractal nanoclusters as the films grow thicker, leading to a giant increase of conductivity before it levels off, see Figure 2a. No continuous electrical pathway has formed at this stage, and thermally activated tunneling dominates the charge transport. At very high metal concentration, metallic nanoclusters are able to initiate and accomplish the percolation process and eventually form the metallic continuum. This continuous metallic pathway leads to a second rapid increase in conductivity and the switch to Ohmic electron transport. The resulting conductivity is lower than that of pure metallic films due to the presence of dielectric polymer inclusions which significantly reduce the electron mean free path. Figure 2b shows the respective data for the addition of P3HT or PCBM.

iii. Thermal Evaporation of P3HT and PCBM

We demonstrated that P3HT can be thermally evaporated in vacuum and that its chemical composition and structures are largely conserved as confirmed by FTIR and XPS characterization. PCBM is much more difficulty to evaporate than P3HT, even though PCBM consists of small molecules, in contrast to the large P3HT polymer molecules. The evaporation heating power varies from several watts to tens of watts, making it difficult to control this process. PCBM is a derivative of C_{60} with a side chain to increase solubility in solution processing. Figure 3 shows the infrared spectra of a vapor phase deposited PCBM film on KBr substrate and PCBM powder on a KBr pellet in the region from 4000 to 500 cm^{-1}.

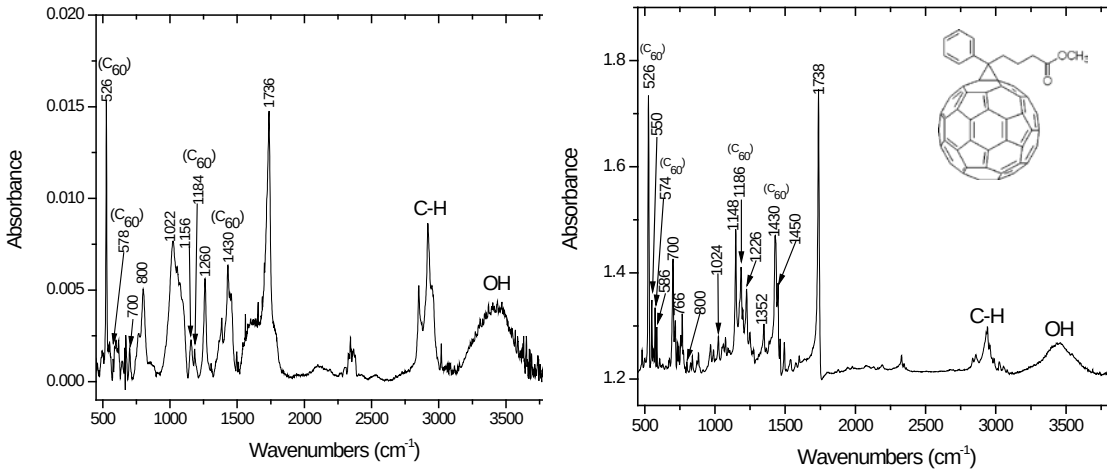

Figure 3. FTIR spectra of PCBM deposited via vacuum thermal evaporation (left). FTIR spectra of as-received PCBM powder on a KBr pellet (right).

The infrared spectra of PCBM are complicated due to the numerous absorption bands present. Although there are intensity variations for IR absorption bands, the major characteristic peaks of PCBM show a one-to-one correspondence for the absorption peak positions. The four strong lines at 526, 576, 1182 and 1428 cm^{-1} provide a characteristic spectral identification for the molecules as C_{60} moieties. The two IR absorption bands at 1735 and 1260 cm^{-1} are associated

with a methyl ester band and an asymmetric stretching of the C-C and C-O bonds attached to the carbonyl carbon [1], confirming the presence of side chains of PCBM.

iv. Interfacial electronic structure of P3HT thin films on Ag substrates

The interfacial and electronic properties of P3HT thermally deposited on polycrystalline Ag foils were studied with XPS and UPS using an *in-situ* deposition technique to prevent potential surface contamination. UPS spectra exhibit an increasing vacuum shift with P3HT layer thickness for initial deposition cycles as measured at the secondary-electron cutoff. This shift is caused by the formation of an interface dipole eD and band bending which increases with polymer layer thickness. The band bending taking place at the polymer/metal interface is also manifested in the XPS measurements by the binding energy shift for both C 1s and S 2p peaks. Finally, the localized π-band energy position shifts as a function of P3HT layer thickness to saturate around 2 nm coverage. The value of the hole injection energy is estimated to be 0.6 eV which places P3HT in the *p*-type material category consistent with previous work of P3HT deposited by spin coating and electrospray methods. Figure 4 schematically summarizes the correlative energy levels at the interface of P3HT/Ag.

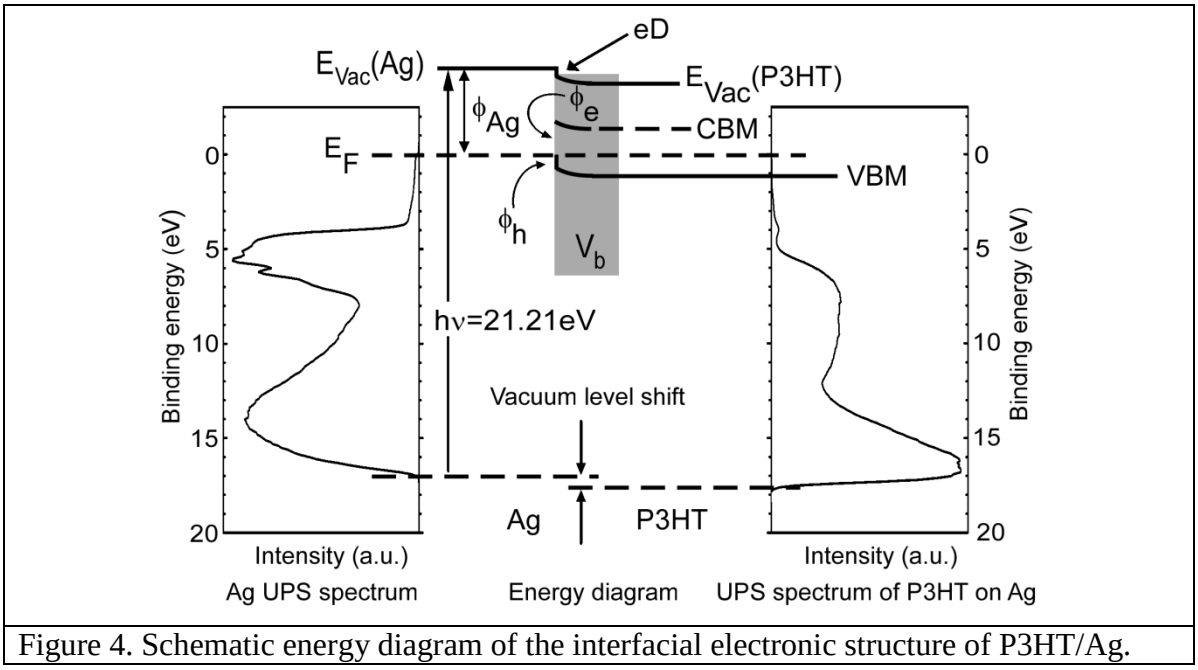

Figure 4. Schematic energy diagram of the interfacial electronic structure of P3HT/Ag.

v. Interfacial electronic structure of Ag/P3HT nanocomposites

Chemical, electronic and structural information were obtained on vapor-phase co-deposited Ag/P3HT nanocomposites with variation of metal content. Ag exists in the form of nanoparticles embedded in P3HT matrix as confirmed by AFM images. Composites with low metal content exhibit a decrease in electrical conductivity due to the spatial distribution of the metal phase which changes the $V_{interface}/V_{particle}$ ratio. XPS indicates that there are at least two chemical bonding states between Ag and S in P3HT. UPS measurements show some similarity in the derived region (0 - 5 eV) with the conventional layered structures (P3HT on top). Large secondary cutoff edge shifts (Δ) to higher binding energies were observed with increasing P3HT content. This is mostly due to the vast interfacial areas between Ag nanoparticle/P3HT where the third phase of Ag-S complex resides. The magnitude of HOB edge (barrier height) increases with

polymer content which impedes the charge injection from the Fermi energy of Ag into the valence band of the composite materials. Furthermore, we have demonstrated in this work that it is possible to tune the value of the barrier height (ε_v^F) from 0.55 to 1.36 eV by simply varying the composition of the blend film (Ag/P3HT ratio ranging from 3:1 to 1:3) and changing the electronic properties of nanocomposite materials, see Figure 5. Finally, three small yet clear peaks were observed in the 5-12 eV region which is related the σ-states of P3HT backbone indicating the possible ordering of these vacuum thermally evaporated polymers as a result of thermal annealing.

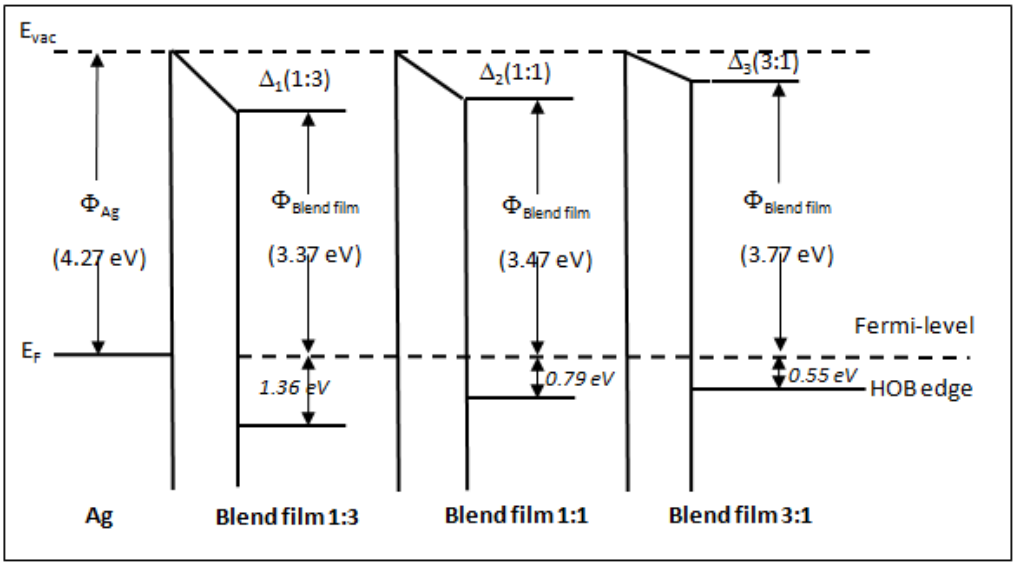

Figure 5: Schematic energy diagram of the interfacial electronic structure of P3HT-Ag nanocomposite as a function of Ag content.

b. Initial Device Performance

A few preliminary reference and active device structures were fabricated and tested, including P3HT:PCBM based structures and Grätzel-cell type structures, see Appendix A. The expectation is that the presence of nanophase silver (n-Ag) in the active structure will increase the range of absorbed wavelengths, similar to what is shown in Figure 1a. Optical absorption spectra were measured for a typical range from 350 nm to 2500 nm. In addition, I-V curves were measured to determine the performance of such device structures. Optical filter were used to select certain wavelength ranges for the I-V measurements.

P3HT:PCBM based reference and active device structures, as well as Grätzel-cell type based reference and active structures were fabricated and their optical and electrical properties measured. The reference structures for both types showed the expected optical absorption in the visible wavelength range and the electrical performance was similar to results reported in the scientific literature. All of the active devices showed increased optical absorption in the near-infrared. The active device structures based on P3HT:PCBM showed an electrical short and no I-V measurements were possible. The active device structures based on the Grätzel-cell design were fabricated with either Ag, Au, or Ag:Au. Spin-coating and thermal evaporation techniques were used to prepare the nanophase metal. However, in none of the cases did the additional metal-based absorption in the near-infrared lead to an increased electrical response.

To better understand the results presented above, we deposited a 30 nm thick layer of silver nanoparticles onto different substrates: glass, glass/ITO, glass/TCO/TiO_2, and glass/ITO/ PEDOT:PSS, and measured the optical absorption of these films, see Figure 6. While the silver film deposited on glass showed the expected broad absorption profile, all other samples showed broad absorption peaks and valleys. These differences can be understood by considering the differences in surface quality (surface energy and roughness) and related morphology of the different substrates.

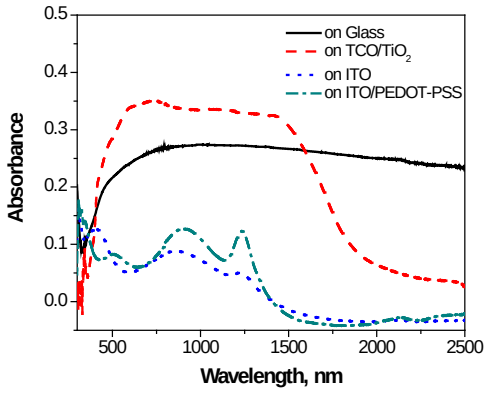

Figure 6. Optical absorption spectra of a 30 nm thick film of silver nanoparticles deposited onto different substrates.

c. Conclusions

- Metallic nanoparticles increase optical absorption range into near-infrared.
- Morphology of metallic nanoparticles depends strongly on substrate and other layers, leading to a large variation in optical absorption.
- Electronic interface structure between nanophase silver and P3HT does not indicate any problems for proposed electronic transfer.
- However, metallic nanoparticles in Grätzel-cell type structures do not appear to lead to the conversion of infrared photons into an electrical signal. Most likely, this is due to a fast recombination of electrons and metallic nanoparticles at the TiO_2/metal interface.

VI. BIBLIOGRAPHY

1. H. B. Liao, R. F. Xiao, J. S. Fu, P. Yu, G. K. L. Wong, and Ping Sheng, "Large third-order nonlinearity in Au:SiO_2 composite films near the percolation threshold," *Appl. Phys. Lett*. 70, 1 (1997).
2. S. Ducourtieux, S. Gresillon, A. C. Boccara, J. C. Rivoal, X. Quelin, P. Gadenne, V. P. Drachev, W. D. Bragg, V. P. Safonov, V. A. Podolskiy, Z. CV. Ying, R. L. Armstrong, and V. M. Shalaev, "Percolation and fractal composites: Optical studies," *J. Nonlin. Opt. Phys. Mater*. 9, 105 (2000) and references therein.
3. Prem Kiran, B. N. Shivakiran Bhkatha, D. Narayana Rao, "Nonlinear optical properties and surface-plasmon enhanced optical limiting in Ag–Cu nanoclusters co-doped in SiO_2 Sol-Gel films," *J. Appl. Phys*. 96, 6717 (2004).
4. M. Westphalen, U. Kreibig, J. Rostalski, H. Lüth, and D. Meissner, "Metal cluster enhanced organic solar cells," *Solar Energy Materials & Solar Cells* 61, 97 (2000).
5. M. Shalaev, in *Optical Properties of Nanostructured Random Media*, (*Topics Appl. Phys*. 82), edited by V. M. Shalaev, (Springer-Verlag Berlin Heidelberg, 2002) pp. 93-114.
6. U. Kreibig and M. Vollmer "Optical Properties of Metal Clusters," Springer Series in Materials Science 25, Springer-Verlag Berlin Heidelberg New York, 1995.
7. D. A. Genov, A. K. Sarychev, and V. M. Shalaev "Metal-dielectric composite filters with controlled spectral windows of transparency," J. Nonlin. Opt. Phys. Mater. 12, 419 (2003).

VII. APPENDIX

Device Structure Results

Several reference (without n-Ag) and active (with n-Ag) device structures, based on either P3HT:PCBM or the Grätzel-cell type were fabricated and tested. The expectation is that the presence of nanophase silver (n-Ag) in the active structure will increase the range of absorbed wavelengths, similar to what is shown in Figure 2a, and lead to conversion of infrared light into an electrical signal. The structures were fabricated using a combination of spin-coating and thermal evaporation.

A. Device Structures based on P3HT:PCBM

Reference Structure

Figure 7a shows the absorption spectrum of an active layer consisting of P3HT:PCBM. This is a well-known material combination that is actively investigated for organic solar cell applications. Figure 7b shows the I-V curve for this reference structure, showing a short-circuit current density of J_{SC} = 0.169 mA/cm^2 and open-circuit voltage of V_{OC} = 0.527 V.

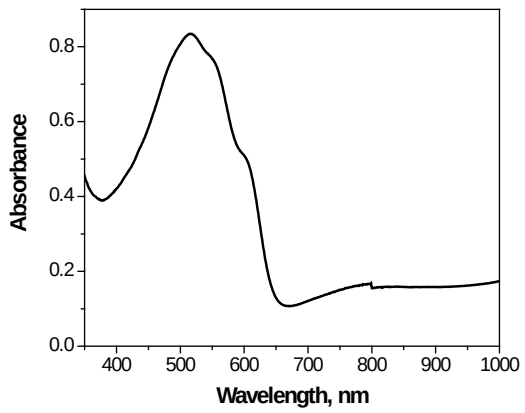

Figure 7a. Optical absorption spectrum of P3HT:PCBM active layer.

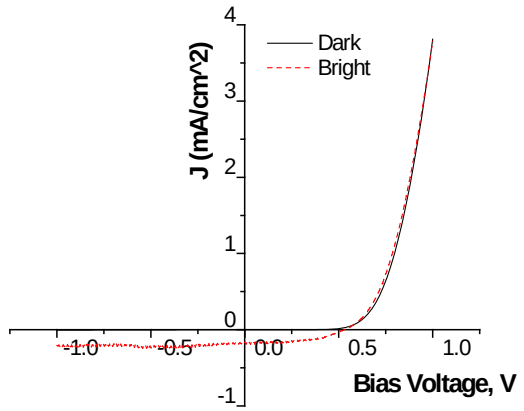

Figure 7b. I-V Curves of ITO/PEDOT:PSS/ P3HT:PCBM/Al illuminated with a 60 W light bulb over a 1 cm^2 active area.

Active Device Structures with n-Ag

To test the effect of incorporating nanophase silver into a P3HT:PCBM assembly, the device structures shown in Figures 8 and 9 were fabricated.

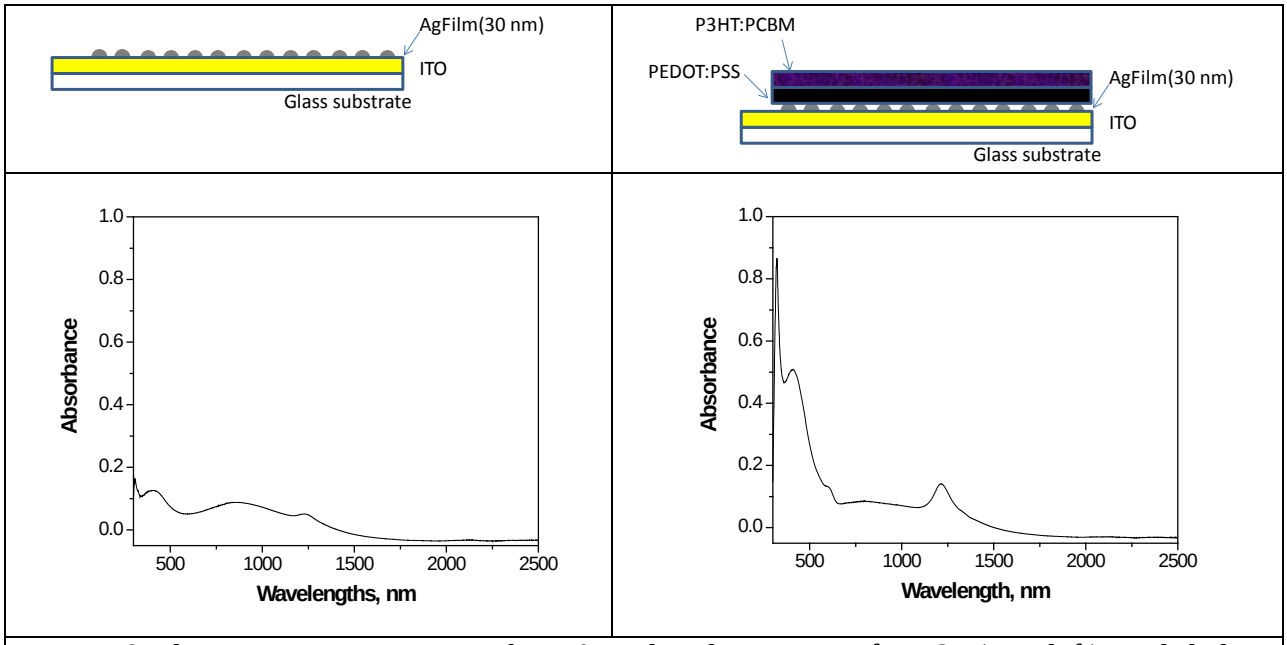

Figure 8a-d. Device structures with n-Ag placed on top of ITO (top left) and below PEDOT:PSS/P3HT:PCBM (top right) and their respective optical absorption spectra. In both cases, a glass/ITO structure served as the reference.

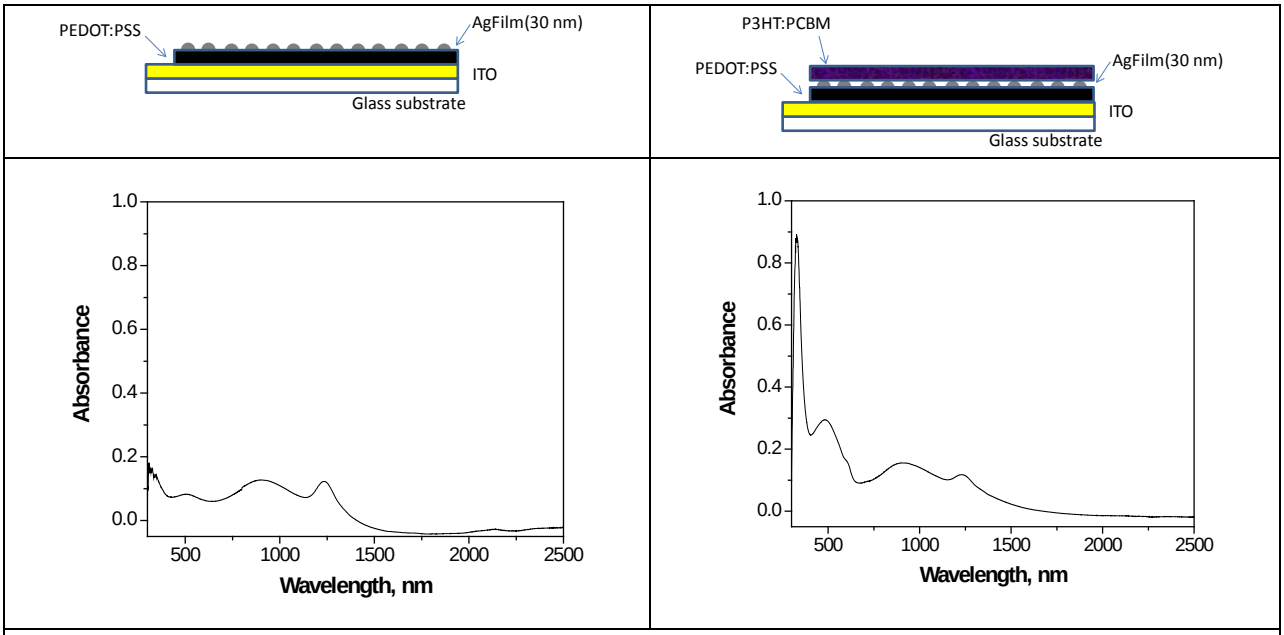

Figure 9a-d. Device structures with n-Ag placed on top of ITO/PEDOT:PSS (top left) and below P3HT:PCBM (top right) and their respective optical absorption spectra. A glass/ITO/ PEDOT:PSS structure (left) and a glass/ITO structure (right) served as the reference.

As can be seen from Figures 8 and 9, the inclusion of nanophase silver (n-Ag) extends the optical absorption range into the near infrared region. All of the active device structures we prepared showed an electrical short, making I-V measurements impossible. Since this electrical short only occurred with the active structures, but not the reference structures, its cause appears to be related to the introduction of nanophase silver particles into the structures.

B. Device Structures based on Grätzel Cell Design

To determine whether metallic nanoparticles can enhance the absorption range of Grätzel-cell-type devices, various device structures were fabricated and characterized:

Reference Structure

The reference structures consisted of either a TCO-coated glass substrate, a thin coating of TiO_2 nanoparticles, a KI/I electrolyte, a carbon layer, and another TCO-coated glass substrate as the counter electrode, or a similar structure with a molecular dye adsorbed on the surface of the TiO_2 nanoparticles, Figure 10.

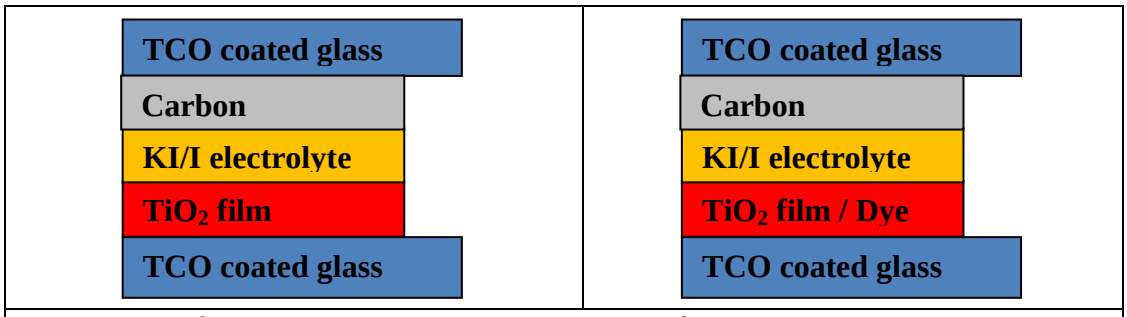

Figure 10. Reference structure without activator (left) and with dye activator (right).

Figure 11 shows the I-V measurement results under different conditions for the structure shown in Figure 6a (no activator material). Any response appears to be due to the direct absorption of UV light by TiO_2.

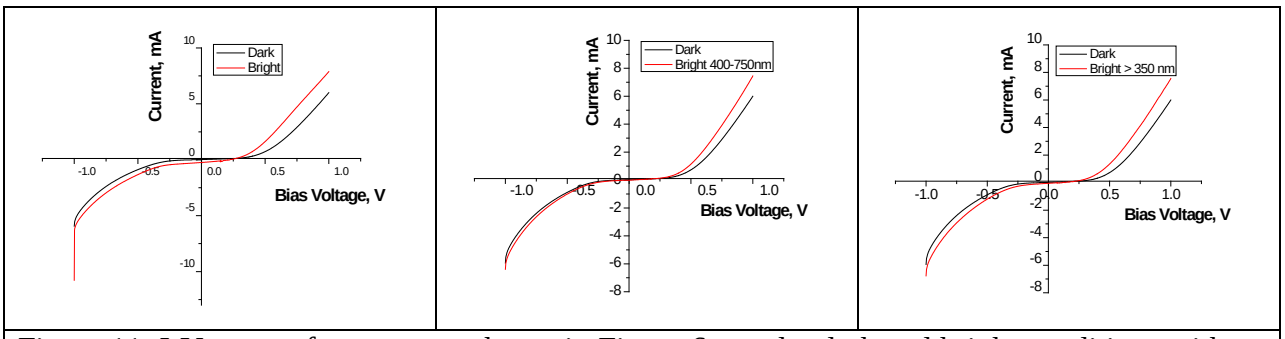

Figure 11. I-V curves for structure shown in Figure 6a, under dark and bright conditions with no optical filters (left), under dark and bright conditions with a 400-750 nm bandpass filter (center), and under dark and bright conditions with a 350 nm long-pass filter (right).

Figure 12a shows the optical absorption spectrum, indicating the typical absorption in the visible wavelength range. Figure 12b shows three I-V curves for this device, without light (Dark), using a 150 W Quartz Halogen sources (Bright), and using the 150 W Quartz Halogen sources with an 850 nm long-pass filter. Without the filter, a short-circuit current density of J_{SC} = 0.920 mA/cm^2 and an open-circuit voltage of V_{OC} = 0.490 V were measured. As expected, the device does not function with the filter (using only NIR light) in place.

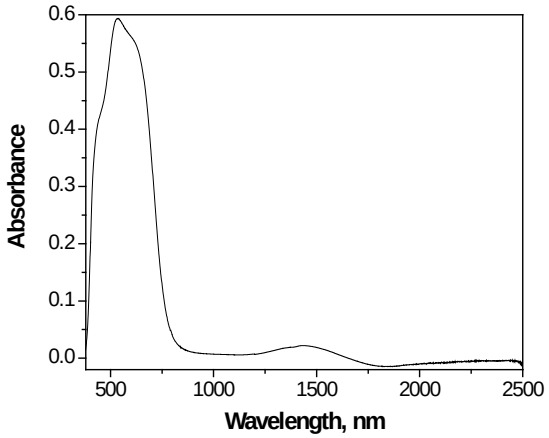

Figure 12a. Optical absorption spectrum of Blackberry dye on TCO/TiO_2.

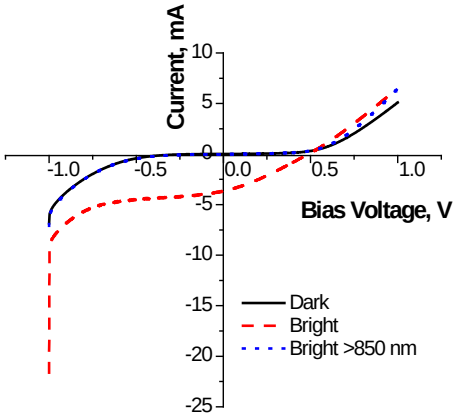

Figure 12b. I-V Curves in dark, bright (150W Quartz Halogen Source), and blocked with a > 850 nm optical filter conditions. The active area is 4 cm^2.

Grätzel cell containing AgNPl@TiO_2.

To determine whether silver nanoparticles might be able to enhance the NIR absorption and lead to increased conversion efficiencies, we incorporated silver nanoparticles in the form of nanoplatelets coated with TiO_2 (AgNPl@TiO_2) into the Grätzel cell design, Figure 13.[2] The TiO_2 coating of the silver prevents the corrosion of the metal by the electrolyte during the electro-chemical reaction.[3]

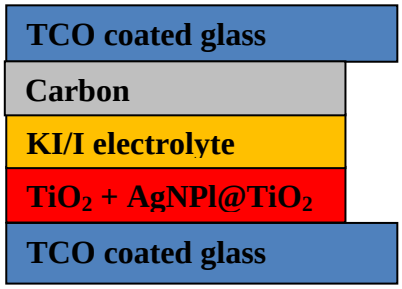

Figure 13. Grätzel cell design containing AgNPl@TiO_2.

Figures 14a and 14b show SEM images of the AgNPl without and with the TiO_2 coating. The silver nanoplatelets are about 30 nm to 200 nm in diameter. The thickness of the TiO_2 coating is difficult to estimate from the SEM images.

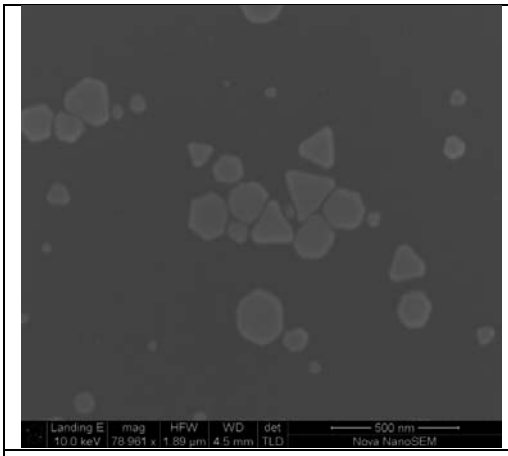

Figure 14a. SEM images of AgNPls

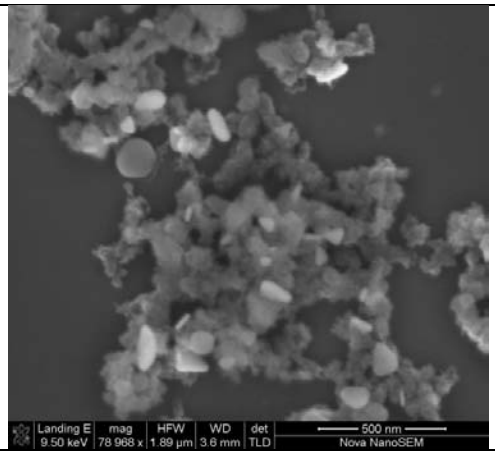

Figure 14b. SEM images of AgNPl@TiO_2

Figure 15a shows the absorption spectrum of this device structure, indicating that the silver nanoplatelets absorb in the visible and near-infrared. Figure 15b shows three I-V curves, without light (Dark), using a 150 W Quartz Halogen sources (Bright), and using the 150 W Quartz Halogen sources with an 850 nm long-pass filter, for this device. Without the filter, a short-circuit current density of J_{SC} = 0.180 mA/cm^2 and an open-circuit voltage of V_{OC} = 0.310 V were measured. However, even though the absorption now extends into the near-infrared range, no electrical current is observed when an 850 nm long-pass filter is used.

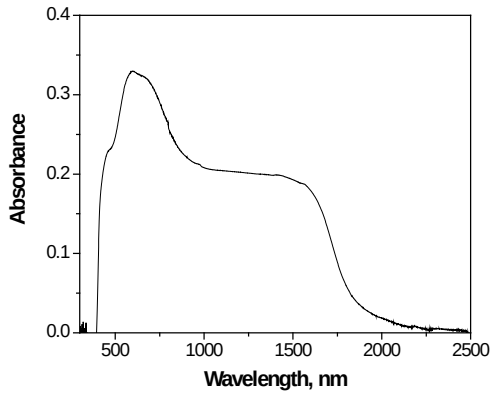

Figure 15a. Optical absorption spectrum of TCO/AgNPl@TiO_2.

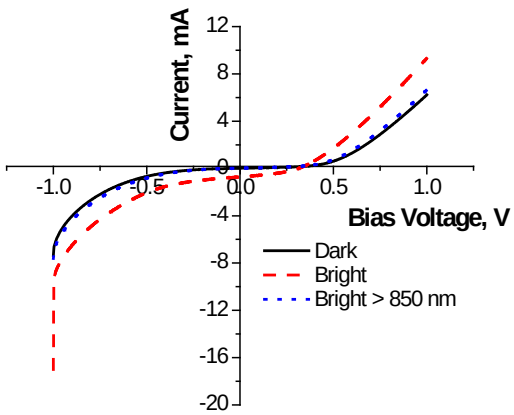

Figure 15b I-V Curve in dark, bright (150W Quartz Halogen Source), and blocked with a > 850 nm optical filter conditions. The active area is 4 cm^2.

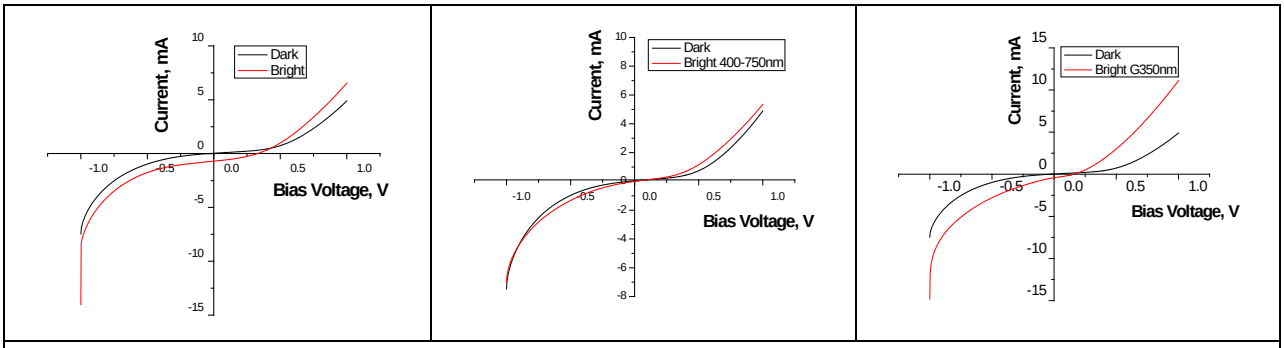

Figure 16. I-V curves for structure shown in Figure 13, under dark and bright conditions with no optical filters (left), under dark and bright conditions with a 400-750 nm bandpass filter (center), and under dark and bright conditions with a 350 nm long-pass filter (right).

Grätzel cell containing Ag-AuNPl@TiO_2.

To determine the effect of the metal on the device performance, we also characterized device structures that contain nanophase gold. In our first attempt, we used a galvanic exchange with $HAuCl_4$ reaction to synthesize bimetallic Au-AgNPl (left).[4] Figure 17a shows an SEM image of Au-AgNPl, and Figure 17b shows an SEM image of Au-AgNPl@TiO_2.

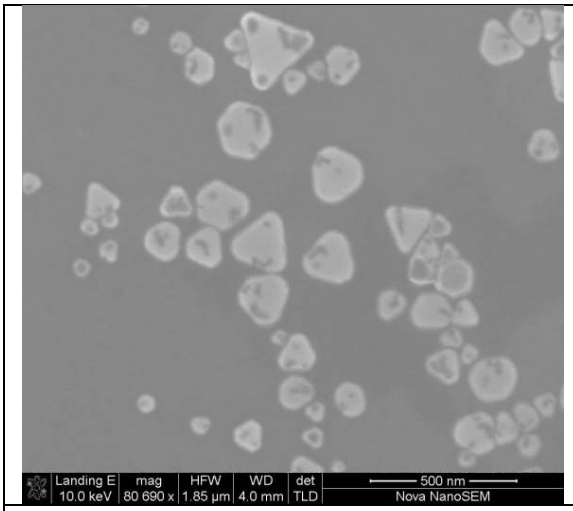

Figure 17a. SEM image of Au-AgNPl

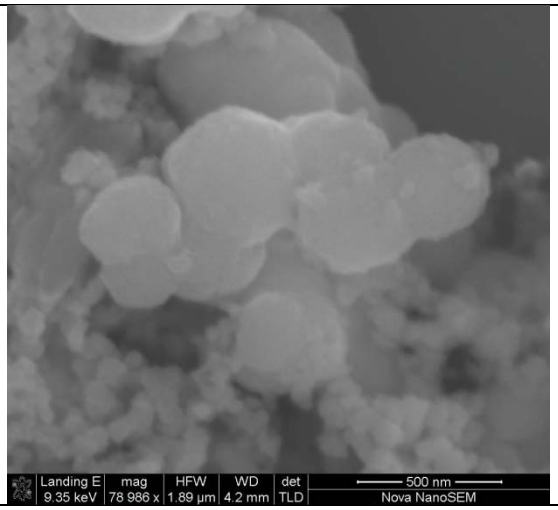

Figure 17b. SEM image of Au-AgNPl@TiO_2

Figure 18a shows the optical absorption of Au-AgNPl@TiO_2, indicating a similar range as AgNPl@TiO_2 shown in Figure 15a. Figure 18b shows three I-V curves, without light (Dark), using a 150 W Quartz Halogen sources (Bright), and using the 150 W Quartz Halogen sources with an 850 nm long-pass filter, for this device. Without the filter, a short-circuit current density of only J_{SC} = 0.079 mA/cm^2 and an open-circuit voltage of V_{OC} = 0.261 V were measured. While the absorption extends into the near-infrared range, similar to the pure Ag, no electrical current is observed when an 850 nm long-pass filter is used. Also, the I-V signal from the visible light for the Ag-Au alloy has decreased compared to the pure Ag, indicating that silver performs better than gold.

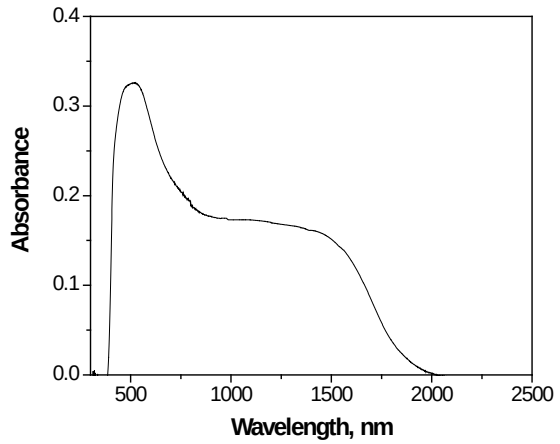

Figure 18a. Optical absorption spectrum of Au-AgNPl@TiO_2.

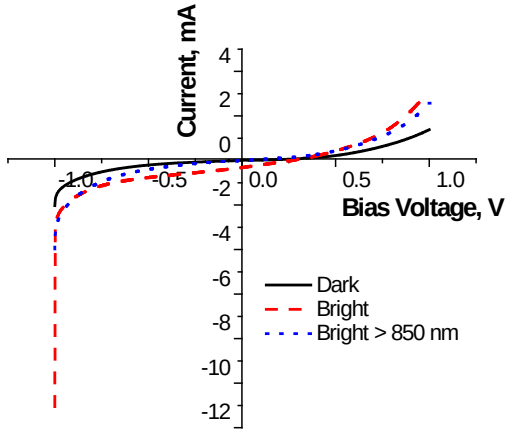

Figure 18b. I-V Curves in dark, bright (150W Quartz Halogen Source), and blocked with a 850 nm optical long-pass filter. Active area is 4 cm^2.

Grätzel cell with thermally evaporated gold nanoparticles

To determine the effect of deposition technique on the device performance, we fabricated Grätzel-cell type structures in which we deposited gold or silver nanoparticles by thermal evaporation, see Figures 19a and 19b.

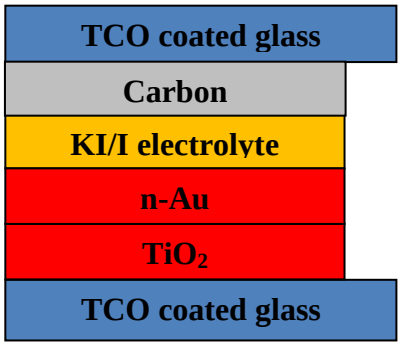

Figure 19a. Grätzel cell design containing thermally-evaporated n-Au on TiO_2.

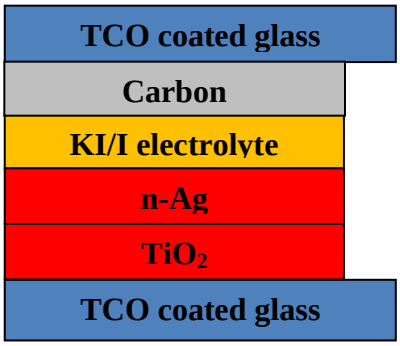

Figure 19b. Grätzel cell design containing thermally-evaporated n-Ag on TiO_2.

Figure 20a shows the I-V curves, without light (Dark) and using a 150 W Quartz Halogen sources (Bright) for the n-Au-based device. A short-circuit current density of only J_{SC} = 0.035 mA/cm^2 and an open-circuit voltage of only V_{OC} = 0.045 V were measured for the n-Au-based device structure. These measurements confirm that gold is not a suitable choice for this device structure and that thermal evaporation results an inappropriate distribution of the gold particles.

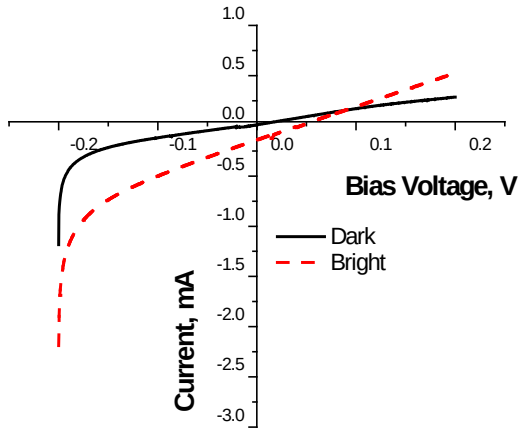

Figure 20a. I-V Curves in dark and bright (150W Quartz Halogen Source) conditions.

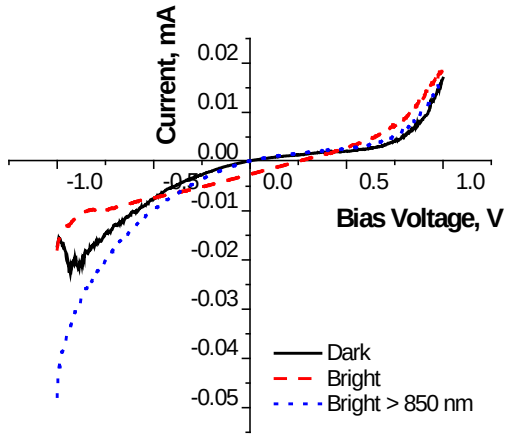

Figure 20b. I-V Curves in dark, bright (150W Quartz Halogen Source), and blocked with a 850 nm optical long-pass filter. Active area is 4 cm^2.

Figure 20b shows three I-V curves, without light (Dark), using a 150 W Quartz Halogen sources (Bright), and using the 150 W Quartz Halogen source with an 850 nm long-pass filter, for the n-Ag-based device. Without the filter, a short-circuit current density of only about J_{SC} = 0.005 mA/cm^2 and an open-circuit voltage of V_{OC} = 0.257 V were measured. No electrical current is observed when an 850 nm long-pass filter is used. Also, the electrical current observed under visible light illumination is very low.

To better understand the results presented above, we deposited a 30 nm thick layer of silver nanoparticles onto different substrates: glass, glass/ITO, glass/TCO/TiO_2, and glass/ITO/ PEDOT:PSS, and measured the optical absorption of these films, see Figure 21. While the silver film deposited on glass showed the expected broad absorption profile, all other samples showed broad absorption peaks and valleys.

These differences can be understood by considering the differences in surface quality (surface energy and roughness) and related morphology of the different substrates. Figure 22 shows SEM images of the n-Ag films on different substrates.

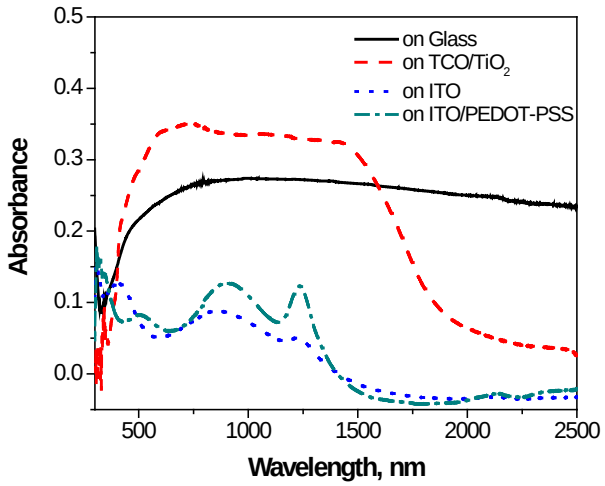

Figure 21. Optical absorption spectra of a 30 nm thick film of silver nanoparticles deposited onto different substrates.

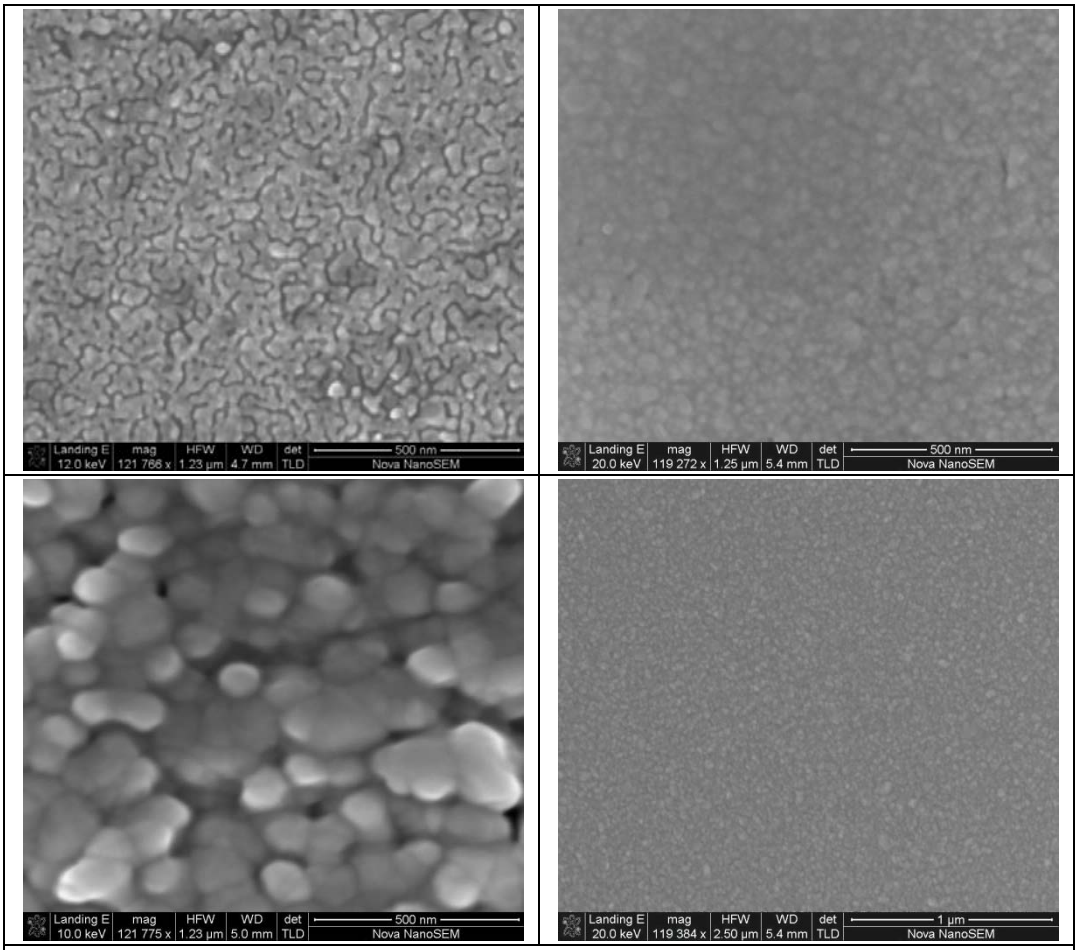

Figure 22. SEM images of 30 nm thick n-Ag film on glass (top left), ITO (top right), TiO_2 (bottom left), and PEDOT:PSS (bottom right) substrates.

References

[1] B. Smith, *Infrared Spectral Interpretation: A Systematic Approach* (CRC Press, Boca Raton, FL, 1999).

[2] X. He, and X. J. Zhao, Applied Surface Science **255**, 7361 (2009).

[3] S. D. Standridge, G. C. Schatz, and J. T. Hupp, Langmuir **25**, 2596 (2009).

[4] Y. G. Sun, B. T. Mayers, and Y. N. Xia, Nano Letters **2**, 481 (2002).